

Growth rates of viscoelastic vortex rings

Judit Clopés Llahí

*Facultat de Física, Universitat de Barcelona, Martí i Franquès 1, 08028 Barcelona, Spain.**

(Dated: June 16, 2014)

Abstract: In this research, experimental studies were performed to investigate the mechanisms of vortex ring formation in a viscoelastic solution of CPyCl/NaSal [100:60] mM in distilled water. We used 2-dimensional particle image velocimetry (PIV) to characterize the transition from laminar to unstable regimes in a cylindrical oscillatory pipe flow, for a constant frequency of 5 Hz. Measurements reveal that the activation time of the vortex rings shows a dramatic dependence with the forcing amplitude, in contrast with the development time of the vortex rings, which seems to be independent of the forcing amplitude and remains constant with a value of 1.9 ± 0.5 s.

I. INTRODUCTION

Complex fluids, and particularly viscoelastic fluids, are found in many systems of interest. More concretely, oscillatory flows of this kind of fluids inside pipes or tubes are present in engineering processes such as fluid pumping or filtration. Also, in physiology, pulsating flow dynamics controls important processes like blood circulation and respiration [1].

Complex fluids differ from newtonian fluids in the mechanic response against applied stresses and strain rates. While newtonian fluids show a linear response to strain rates or stresses, complex fluids react with a non-linear behaviour. Viscoelastic fluids act as a solid material on short time scales -below their characteristic relaxation time-, but flow like a viscous fluid on longer time scales. This behaviour is a consequence of the interaction between the flow and the fluid microscopic structure.

The fluid used to perform these experiments is a CPyCl/NaSal [100:60] mM aqueous surfactant solution. This fluid contains cationic surfactant molecules, which are amphiphilic and spontaneously self-assemble to generate cylindrical long aggregates called wormlike micelles. The dynamics of wormlike micellar systems differs from those of conventional polymer chains in that micellar systems are continuously breaking apart and recombining.

CPyCl/NaSal [100:60] mM is a canonic fluid for small shear rate values ($\dot{\gamma}$), but for increasing $\dot{\gamma}$ the fluid presents shear-thinning, e.g. the resistance against external strain rate diminishes drastically. This behaviour is a consequence of the reorientation of the wormlike micelles with the flow. For small shear rate values, this fluid follows the behaviour of a typical Maxwell fluid.

Oscillatory forcings test the fluid behaviour for a varying acceleration. It is known that, for periodic drivings, the CPyCl/NaSal [100:60] mM aqueous solution self-structures in three differentiate regimes depending on the frequency and the amplitude of the driving: laminar, axisymmetric-vortical and turbulent. Laminar regime is characterized by a translational symmetry along the di-

rection of the driving and the lack of transversal component of the velocity. In this regime, the solution is structured in concentric cylindrical domains of fluid masses moving in opposite velocities. The axisymmetric-vortical regime, in contrast, shows a breaking of the translational symmetry due to the appearance of characteristic vortex rings in determined positions respect the origin of the forcing. The cylindrical symmetry is still preserved, and the total number of vortex rings depends on the height of the fluid column. These vortex rings appear in the regions where $\dot{\gamma}$ is maximum. For high forcings and/or frequencies, the fluid enters to the turbulent regime, where all symmetries are broken and there are no specific patterns for the velocity field. An interesting property of the response of the fluid against an oscillatory driving is the resonance phenomena. Resonance occurs for well defined frequencies depending on the geometry of the setup, and are a consequence of the constructive interference of the viscoelastic waves generated by the pressure gradient [2]. In our analysis, we have worked at non-resonant frequencies.

Growth rates for a constant time phase of the oscillatory driving are a magnitude that allows a numerical analysis of the mechanisms of vortex ring formation. These rates are related with the fluctuations of the velocity field. It is expected to find a significant variation of these fluctuations during the appearance of the vortex rings, and a different profile of the growth rates for periods belonging to different regimes.

Since the frequency and amplitude stability boundaries between these three regimes have already been explored recently by Casanellas and Ortín (2014), it is now a matter of interest to study also the temporal dependence between these regimes on the time scales. In the present analysis, several measurements of typical times involved in the destabilization of the rectilinear oscillatory flow into the axisymmetric-vortical regime have been done. We analyzed the mechanisms of formation of the first vortex ring closer to the piston at a constant oscillatory frequency of 5 Hz, nearly ten times the inverse of the relaxation time of the fluid. Different driving amplitudes from 1.35 mm to 1.94 mm have been considered.

The results obtained will be useful to compare with future experimental results and theoretical predictions on linear flow stability.

*Electronic address: jclope117@alumnes.ub.edu

II. EXPERIMENTAL

A. The wormlike micellar solution

The fluid consists in a surfactant solution of cetylpyridinium chloride (CPyCl, $m_0 = 358$ g/mol) and sodium salicylate (NaSal, $m_0 = 160.1$ g/mol) with a concentration of [100:60] mM diluted in distilled water. The solution contains also a small concentration of tracer particles (0.040 g/l). Rheological properties of this solution are reported in Table I.

η_0 (Pa·s)	ρ (kg/m ³)	λ (s)	$\dot{\gamma}_c$ (s ⁻¹)
64	1050	1.9	0.4

TABLE I: Rheological properties of CPyCl/NaSal [100:60] solution (zero shear-rate viscosity η_0 , density ρ , relaxation time λ and critical shear rate $\dot{\gamma}_c$), all values for a room temperature of 24 °C.

This solution must rest two days after being mixed. Is stable for at least two weeks, and should be protected from ambient light exposition.

B. The experimental setup

The experimental setup is composed mainly of a large cylinder of 5 cm diameter built of transparent methacrylate, containing 1 l of CPyCl/NaSal [100:60] mM aqueous solution, surrounded by a square-based tank filled with glycerin (Fig.1).

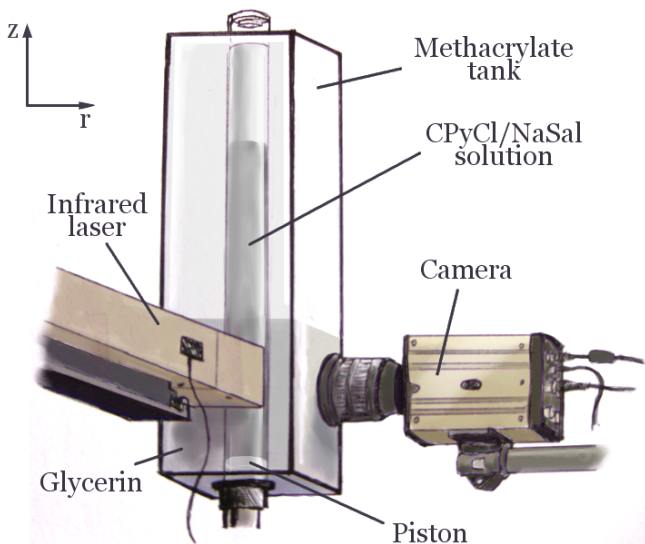


FIG. 1: Sketch of the experimental setup.

The refractive index of glycerin is nearly equal to that of methacrylate, so the cylindrical aberrations are almost eliminated. The laser provides an intense illumination to the fluid, which consists in a vertical sheet of infrared

light pulses passing through a meridional plane of the central region of the cylinder. The camera is synchronized with the laser pulses and, for these measurements, takes a frame every 0.004 s, which means a total of 50 frames per period. Piston amplitude is controlled by a step motor. The amplitude value is set with a maximum precision of 0.04 mm. Step changes in amplitude are limited by the velocity of the step motor, which is of 0.1 mm/s.

The parameters of frame captures are controlled with the commercial software Motion Studio and a home-made program. All the measurement processes are controlled automatically except the constant oscillatory frequency, which is entered manually. In Casanellas and Ortín (2014) previous analysis, they observed a resonance phenomenon at 6.8 Hz and 10.3 Hz. In the present study, we have worked with a non-resonant frequency of 5 Hz.

Remanent aberrations are corrected by a non-linear mapping along r of the studied region. As shown in Fig.2, these aberrations are found to be significant at the edges of the tube, for radii larger than 20 mm.

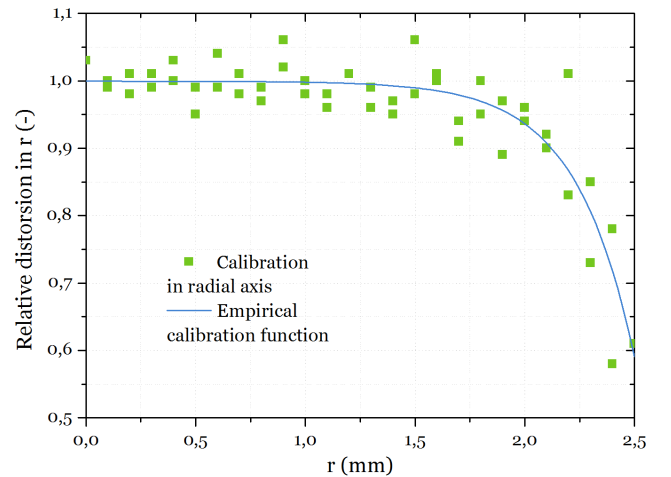


FIG. 2: Correction of the remanent cylindrical aberrations along the radial axis.

C. 2D Particle image velocimetry

The particle image velocimetry (PIV) is a non-intrusive measurement technique to obtain the instantaneous velocity of every tracer particle in a fluid flow [3]. In 2D PIV, azimuthal and radial velocity components are measured in a meridional plane (r, z) of the tube. Data analysis has been done with the VidPIV 4.3 commercial software, that uses a cross-correlation method to provide the velocity fields.

D. Measurement protocol

Two measurement protocols have been applied to obtain all the results in this study (Fig.3). The first protocol consists of maintaining a constant driving of 0.95 mm for 30 s, where the flow is laminar, and then ramp up to a final amplitude belonging to the axisymmetrical-vortical regime. This ramping up occurs in a typical time lapse of around 10 s (t_{A-ramp}). Depending on the measurement, it is possible to wait some time at the final amplitude after starting the camera shots (t_{sleep}). The second protocol consists of starting the driving with the final amplitude set. There is a frequency transient of about 4 s ($t_{\nu-Ramp}$) before the preset frequency of 5 Hz is reached. Shot time (t_{shots}) is the time where the camera is taking frames, and its value is 12 s for both protocols.

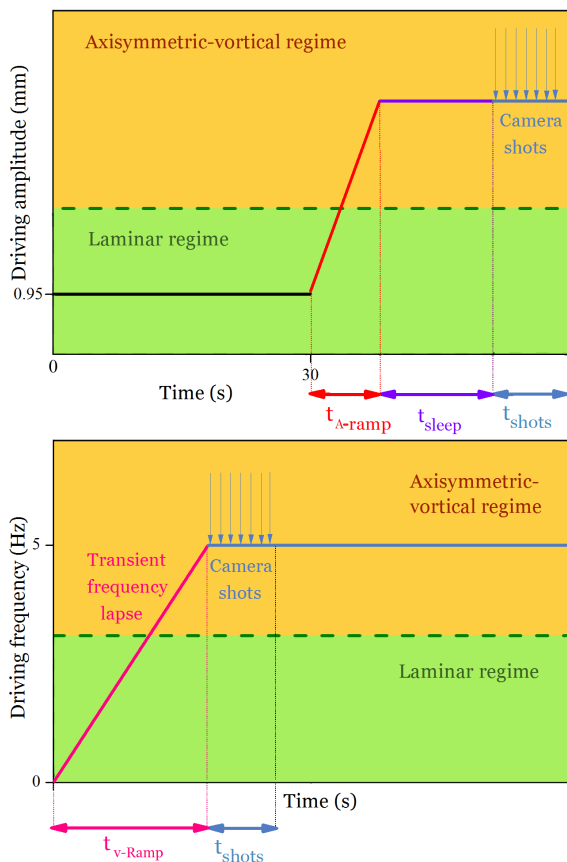


FIG. 3: Measurement protocols used to perform the experiments.

The first protocol has been used for final driving amplitudes below 1.65 mm. However, for driving amplitudes above 1.65 mm, the vortex rings develop during the ramp and cannot be measured with the first protocol. Therefore, the second protocol has been used for measurements above 1.65 mm of final driving amplitude.

The piston temporal phases, $\phi = \omega_0 t$, have been defined as follows: $\phi = 0, \pi$ rad correspond to those phases where the velocity of the piston is maximum and the

acceleration and the amplitude are null. In 0 rad, the piston is moving upwards and in π rad, the piston moves downwards. These points are where the piston begins to decelerate. On the contrary, $\phi = \pi/2, 3\pi/2$ rad are the phases of maximum and minimum acceleration and amplitude respectively. Here, the velocity of the piston is zero.

More data would be needed to state that the two measurement protocols are analog. Ideally, both protocols are expected to be equivalent when the final parameters (frequency and amplitude) are reached.

III. RESULTS AND DISCUSSION

The formation of vortex rings in an oscillatory flow is a consequence of the viscoelastic nature of the solution. During the laminar regime, the velocity field ($u_z(r, z, t), u_r(r, z, t)$) presents a quasi-translational symmetry in z for every time phase, e.g., $u_z \approx u_z(z_i)$ for a fixed r . In addition, u_r is negligible during laminar regime. However, for a given phase, there exists a small difference between the velocity u_z near the piston and in the region of the top of the fluid column, due to the time needed for the fluid to propagate the velocity within. This difference, if it overcomes the amount dissipated due to the viscosity of the fluid, is being accumulated every period, until the system cannot compensate this. Then, a collision between upwards and downwards fluid masses is produced when the piston reaches the maximum acceleration in the period. During the collision, the mass with less absolute velocity bends out to larger radii regions to let the fastest mass pass through. Hence, $\langle u_r \rangle$ increases. These first collisions belong to the transition between laminar and axisymmetric-vortical regime, because vortex rings are created and eliminated depending on the piston acceleration. During the transition, the velocity field of these vortex rings show a nearly circle-shaped bending, in which $\langle u_z \rangle$ and $\langle u_r \rangle$ reach values of the same order of magnitude. When vortex rings are completely formed, its velocity field (u_z, u_r) stretches out in u_z but narrows in u_r , hence $\langle u_r \rangle$ decreases and stabilizes to a small but non-zero value.

Figure 4 shows an example of the velocity field and the vorticity magnitude for time phases $\phi = \omega_0 t$ of 0, $\pi/2$, π and $3\pi/2$ rad in the axisymmetric regime. It is observed that time phases 0 and $3\pi/2$ rad display the inverse patterns of π and $\pi/2$ rad time phases respectively. Because of this time symmetry, phases 0, π rad and $\pi/2, 3\pi/2$ rad are considered analogous for the growth rate calculations in Fig.5. One consequence of this symmetry is that the velocity field of vortex rings follows the period of the forcing amplitude in all measurements and phases.

Root-mean-square fluctuations of the velocity field are related to vortex growth rates. The phase-locked growth rates of the fluctuations of a velocity field for the components in the meridional plane ($u_z(r, z, t), u_r(r, z, t)$) are

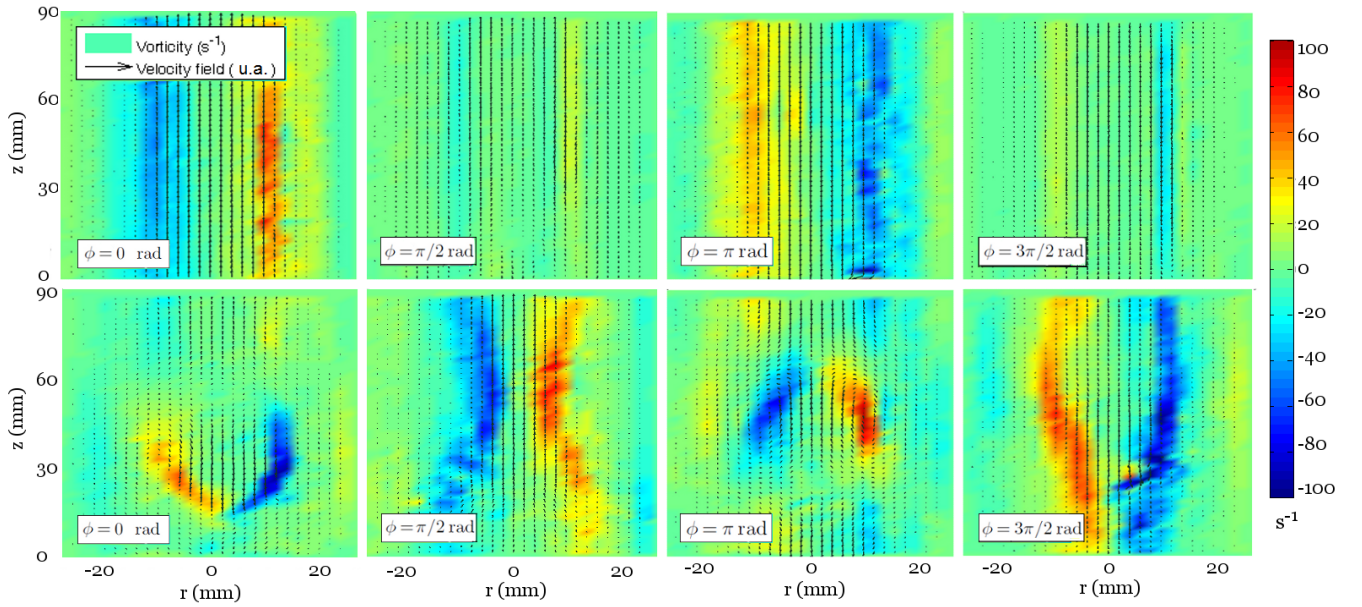


FIG. 4: Velocity field and vorticity magnitude in the laminar regime [top row] and the axisymmetric-vortical regime [bottom row] for time phases 0, $\pi/2$, π and $3\pi/2$ rad, at 0.01 to 0.18 s [top row] and 6.81 s to 6.98 s [bottom row] after ramping, for a forcing amplitude of 1.53 mm.

quantified by the dimensionless magnitude:

$$\langle \sigma_{u_x} \rangle_r = \frac{1}{z_0 \omega_0} \left\langle \sqrt{\frac{1}{N-1} \sum_{i=1}^N [u_x(r, z_i, t) - \bar{u}_x(r, t)]^2} \right\rangle_r \quad (1)$$

where $x = z$ or $x = r$, z_0 and ω_0 are the driving amplitude and the angular velocity of the piston, and $\langle \rangle_r$ corresponds to a radial average. The laminar to vortical regime transition is found to induce a huge variation of the $\langle \sigma_{u_z} \rangle_r$ growth rates at $\phi = \pi$ rad and $\phi = 3\pi/2$ rad and a small variation in $\langle \sigma_{u_r} \rangle_r$ at $\phi = 3\pi/2$ rad, but $\langle \sigma_{u_r} \rangle_r$ for both $\phi = \pi$ rad and $\phi = 3\pi/2$ rad shows a peak during the transition and decreases when the vortex rings are completely formed. This peak is a consequence of the mechanism of vortex ring formation explained at the beginning of this section: when the vortex is being developed, $u_z \gtrsim u_r$, but in the axisymmetrical-vortical regime, $u_z > u_r$. Time phases $\phi = 0$ and $3\pi/2$ rad follow an analog behaviour to $\phi = \pi$ and $3\pi/2$ rad time phases respectively. Figure 5 shows an example of this generic behaviour.

Characteristic time scales are also quantified in this analysis. Three different times are considered: the ramp time is the time needed by the piston to reach the final driving amplitude (t_{A-Ramp}) or frequency ($t_{\nu-Ramp}$), depending on the measurement protocol used in each case; the waiting time (t_{wait}) describes the duration of the laminar regime from the final piston driving amplitude to the beginning of the vortex ring formation, as characterized by a 20% increase of $\langle \sigma_{u_x} \rangle_r$ for $\phi = \pi$ rad, that coincides with the break of the transitional symmetry; and finally, the development time (t_{dev}) quantifies the formation time

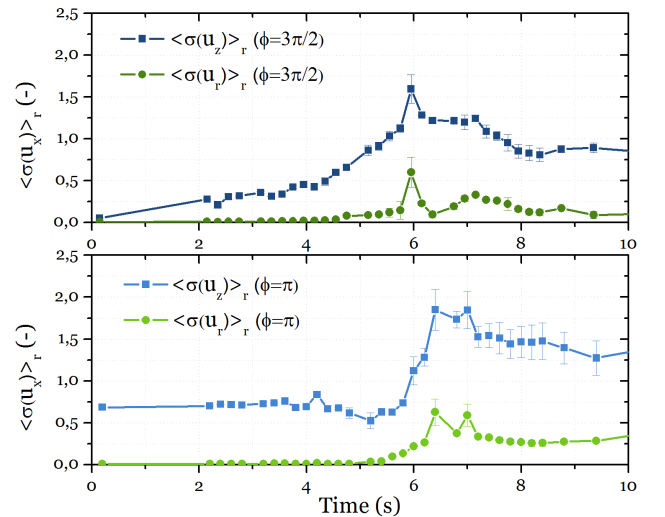


FIG. 5: Growth rates for $\phi = 3\pi/2$ and π rad, for a forcing amplitude of 1.48 mm at a constant frequency of 5 Hz. $t = 0$ corresponds to the instant when the final amplitude is reached, e.g. just after t_{A-Ramp} .

of a complete vortex ring, as characterized by twice the time elapsed from t_{wait} to the peak value of $\langle \sigma_{u_r} \rangle_r$ for $\phi = \pi$ rad.

As shown in Fig.6 [¶], t_{wait} experiences a dramatic

[¶] The linear fitting does not consider the measurements taken with the second protocol.

growth for decreasing amplitudes. This behaviour can be expressed by the following empirical law, extracted from the linear fitting:

$$\frac{1}{t_{wait}} = z_0 \cdot (1.9 \pm 0.2) - (2.5 \pm 0.2) \quad (2)$$

where z_0 is the amplitude of the forcing, expressed in mm, and t_{wait} is expressed in s. However, t_{dev} remains roughly constant (Fig.6), with an average value of 1.9 ± 0.5 s. From these results, it is inferred that vortex ring development time does not depend on driving amplitude. In contrast, t_{wait} exhibits a strong dependence with forcing. The critical driving amplitude for the first vortex over the piston is found to be lower than 1.39 ± 0.04 mm from the measurement of lowest amplitude, and with a value included in 1.3 ± 0.2 mm from Eq.(2), which is consistent with previous results 1.35 ± 0.02 mm for vortices in the middle of the tube [2].

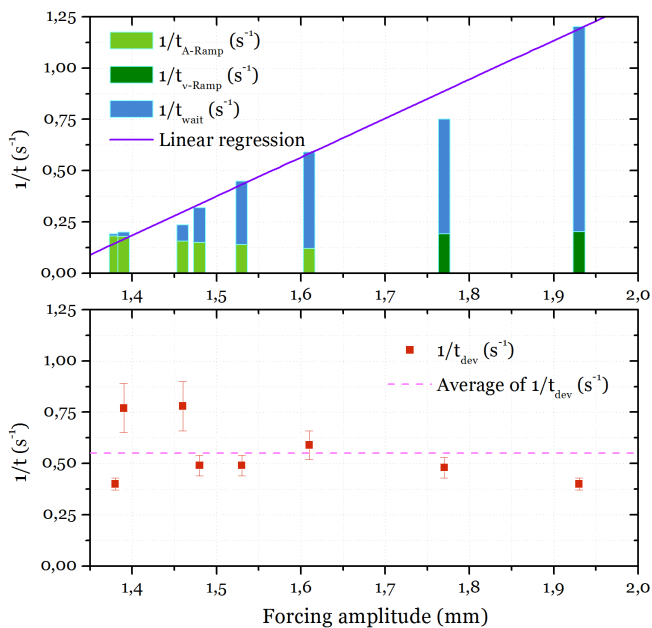


FIG. 6: [Top] Inverse of the characteristic time scales for different forcing amplitudes at a constant frequency of 5 Hz: ramp duration (t_{A-ramp} and t_{v-ramp}), and duration of the laminar regime (t_{wait}). [Bottom] Time of the transition from laminar into axisymmetric vortical regime (t_{dev}).

IV. CONCLUSIONS

- Vortex ring velocity fields in the axisymmetric-vortical regime are antisymmetric for the

($\pi/2, 2\pi/3$) and ($0, \pi$) rad time phases, but completely distinct for the ($\pi/2, \pi$) and ($0, 3\pi/2$) rad time phases. Vortex rings start to form and are more developed at ($\pi/2, 3\pi/2$) than at ($0, \pi$) rad time phases. From these observations, it is deduced that vortex rings are more developed in the time phases of maximum acceleration.

- The dynamics of the system follow the periodicity of the applied driving, both in the laminar and in the axisymmetric-vortical regimes.
- Vortex ring development and characteristic times (t_{dev}) are similar in all measurements. Therefore these processes do not depend on the magnitude of the driving amplitude. Once nucleated, the vortex rings grow in $1.9 \mu\text{s} \pm 0.5$ s, which is equivalent to 9 or 10 time periods of the forcing.
- The characteristic waiting time t_{wait} shows a dramatic increase for lower forcing amplitudes. The dependence between activation time (including the ramp and the waiting time) and forcing amplitude follows the empirical relation (2), that diverges for a critical amplitude of 1.3 ± 0.2 mm. Alternative explanations suggest that the flow could be unstable for any driving amplitude $z_0 \neq 0$ [4], but the divergence of t_{wait} complicates the observation of the formation of vortex rings for small z_0 . For moderate z_0 , t_{wait} values enter within the experimentally accessible time ranges. Finally, for very large z_0 , the vortex rings develop during the ramp and it is not possible to observe them with the experimental setup used in the present study.

Acknowledgments

This work would not have been possible without the encouragement of my advisor Dr. J. Ortín. Many thanks are due to Dra. L. Casanellas for her helpful advice. A special mention to R. Ortiz, for his essential help during the early stages of this work. I would acknowledge A. Comerma for improving the software of the experimental setup. I am very grateful also to R. Aràjol, I. Oliva, G. Arauz, A. Gràcia, and to my parents.

[1] Y. C. Fung, *Biomechanics: Motion, Flow, Stress and Growth* (Springer-Verlag, New York, 1990).
 [2] L. Casanellas and J. Ortín, *J. Rheol.* 58 149-181 (2014).
 [3] M. Raffel et al., *Particle Image Velocimetry. A practical*

guide (Springer, 2nd ed., New York, 2007).
 [4] A. Morozov, *private communication* (2014).